

Reduction of threading defects in GaN grown on vicinal SiC(0001) by molecular-beam epitaxy

M. H. Xie,^{a)} L. X. Zheng, S. H. Cheung, Y. F. Ng, Huasheng Wu, and S. Y. Tong
Department of Physics, The University of Hong Kong, Pokfulam Road, Hong Kong

N. Ohtani

Nippon Steel Corporation, Advanced Technology Research Laboratory, 5-10-1 Fuchinobe, Sagami-hara, 229-8551 Japan

(Received 16 December 1999; accepted for publication 23 June 2000)

We observe a significant reduction of threading dislocations in GaN grown on vicinal substrates of SiC(0001). Using scanning tunneling microscopy, we find films grown on vicinal substrates maintain the surface misorientation of the substrate and display terraces with straight edges. On top of the terraces there is no spiral mound, which is the main feature found for films grown on singular substrates. Transmission electron microscopy studies confirm that threading screw dislocations are reduced by two orders of magnitude while edge dislocations are reduced by one order. © 2000 American Institute of Physics. [S0003-6951(00)00934-7]

In heteroepitaxy, such as GaN on sapphire and SiC, a central concern is the reduction of threading defects traversing the entire thickness of the film. A high density of such defects results in poor film quality. In a typical heteroepitaxial GaN film, the density of threading dislocations is in the range of 10^{10} cm^{-2} .^{1,2} This is at least 10^6 times higher than that found in III-V arsenide or phosphide films. Although the major technique of growing GaN for optoelectronic devices is by metal-organic chemical-vapor deposition (MOCVD), the molecular-beam epitaxy (MBE) technique allows *in situ* diagnostic observations. Certain microscopic processes related to nucleation and growth learned from such *in situ* studies may be applicable to both MBE and MOCVD. Furthermore, MBE-grown films may have good prospects for various photodetectors and electronic devices. In this regard, a reduction of threading dislocations in MBE films is relevant and important. For growth of GaN(0001) on a flat substrate surface, a common growth process is the formation of threading screw dislocations with Burgers vector $\mathbf{b}=\mathbf{c}=[0001]$. This leads to spiral mounds and, consequently, a poor surface morphology of the film.^{3,4}

In this letter, we report direct evidence of integral suppression of spiral mounds and threading dislocations in GaN grown on vicinal 4H-SiC(0001) substrates. Transmission electron microscopy (TEM) studies reveal considerable reduction of both screw- and edge-type threading dislocations compared to films grown on singular substrates. This study thus suggests a potentially useful way of growing high-quality epitaxial films by MBE, and even by MOCVD, as these results seem to be more related to the edge structures in vicinal surfaces than to growth techniques.

The MBE system contains a conventional effusion cell for Ga and a radio-frequency plasma generator (Oxford Applied Research, CARS25) for N. The substrates are 4H-SiC(0001) (Nippon Steel Co.) misoriented towards $[\bar{1}010]$ by 3.5° and nominally flat 6H-SiC(0001) (Cree Research

Inc.). They are thermally deoxidized at 1100°C in a Si flux, which leads to atomically smooth surfaces and a $(\sqrt{3} \times \sqrt{3})R30^\circ$ surface reconstruction. GaN epitaxy is initiated by simultaneously supplying the Ga and N source fluxes under the excess-Ga condition.⁵ The growth rate is approximately 0.26 \AA/s . The substrate temperature is kept at 650°C throughout to ensure a step-flow growth mode. No nucleation or buffer layers are used. Following $0.5\text{-}1 \mu\text{m}$ film deposition, the growth is stopped and the sample is quenched for *in situ* scanning tunneling microscopy (STM) studies at room temperature. A constant tunneling current of 0.1 nA and a sample bias of -3.0 V are chosen for all the STM experiments reported here. Plan-view TEM investigations of the grown samples are carried out in a Philips CM200FEG TEM microscope at 200 keV . The specimens are prepared by mechanical polishing and argon-ion milling from the substrate side.

Initial growth of GaN on both singular and vicinal substrates commences by island formation, as indicated by spotty reflection high-energy electron diffraction patterns. The GaN films grown on both singular and vicinal substrates are of the Ga polarity, as judged by surface reconstruction observations.^{4,5} On the vicinal substrate, the growth quickly changes to two-dimensional after deposition of a couple of bilayer. Figure 1(a) shows a STM image of a GaN surface

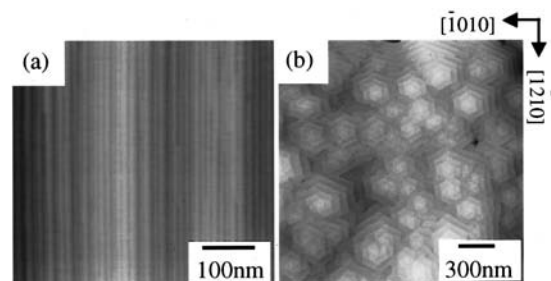


FIG. 1. STM images of GaN surfaces grown on (a) vicinal 4H-SiC(0001) and (b) nominal flat 6H-SiC(0001) substrates under identical growth conditions.

^{a)}Electronic mail: mhxie@hkusua.hku.hk

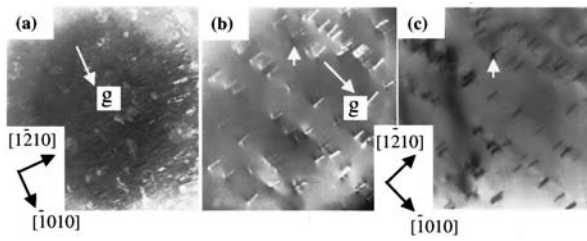


FIG. 2. Plan-view TEM images ($2 \times 2 \mu\text{m}^2$ in size) of GaN films grown on (a) a singular substrate (dark field, $\mathbf{g}=[\bar{2}020]$), (b) a vicinal substrate (dark field, $\mathbf{g}=[\bar{2}020]$), and (c) a vicinal substrate (multibeam bright-field). The images in (b) and (c) are from the same area. The short arrow in (b) and (c) points to a screw dislocation.

following deposition on the 4H-SiC vicinal substrate. It is seen that the epilayer maintains the vicinality of the substrate surface, showing terraces and straight steps. The step height is measured to be double bilayers (i.e., it equals $c = 5.19 \text{ \AA}$ of GaN). The formation of double bilayer steps is a consequence of strong anisotropy in growth rates of type-A and type-B steps of GaN, which has been documented elsewhere.⁶

The most striking observation of Fig. 1(a) is the absence of growth spirals. There is also no sign of step termination, implying an effective suppression of threading screw dislocations in the vicinal film. This contrasts to films grown directly on a singular substrate, where growth spirals are the predominant features.^{3,4} An example of the latter is shown in Fig. 1(b). Spiral mounds, with an average diameter of about 250 nm, decorate the entire surface of the film. From the mound density, it is estimated that the density of threading screw dislocations in such a film is about $2 \times 10^9 \text{ cm}^{-2}$. Zooming in the core regions of the spirals, no hole is revealed, indicating that the dislocations are full-core screws with Burgers vector $|\mathbf{b}| = |\mathbf{c}| = 5.19 \text{ \AA}$.⁷ If a pair of spiral mounds is associated with the two vertical arms of a ‘‘U-shaped’’ dislocation line in the film, the two spirals in the pair ought to have opposite rotation directions, as the Burgers vector of a dislocation line remains unchanged. However, it is noted that the same rotation direction, either clockwise or counterclockwise, is often found for the two nearest spirals. The bilayer growth sheets from different spiral mounds are usually tilted with respect to each other. Therefore, the boundaries where two or more sheets from neighboring mounds coalesce, especially from close-by ones, are likely sources of additional defects. There is evidence from cathodoluminescence microscopy that the most intense yellow luminescence originates from the coalesced boundaries between hexagonal mounds.⁸ Thus, the suppression of screw dislocations in a vicinal film has the additional benefit that the coalescent boundaries of spiral mounds are eliminated at the same time.

It is important to verify that the disappearance of spiral mounds on the vicinal film indeed suggests an absence of screw dislocations. This is necessary because it is possible that the number of dislocations remains the same but only spiral growth on the vicinal surface is inhibited.³ We have carried out plan-view TEM investigations of the same samples. Figure 2 shows two-beam dark-field images of (a)

the film grown on a singular substrate and (b) grown on a vicinal substrate. Figure 2(c) shows, on the other hand, a multibeam bright-field image from the same location as in (b). In all the TEM measurements, the specimen is tilted 50° towards $[1\bar{2}10]$ with respect to the electron beam. Therefore, the dislocation segments observed in the images are, in fact, vertical (along $[0001]$) threading dislocations. Since screw dislocations are out of contrast in the two-beam dark-field images ($\mathbf{g}=[\bar{2}020]$), the dislocation lines shown in Figs. 2(a) and 2(b) are all edge type. From Fig. 2, we estimate the density of edge-type threading dislocations in films grown on singular substrates is $\sim 2 \times 10^{10} \text{ cm}^{-2}$, while that in the vicinal film is $\sim 1 \times 10^9 \text{ cm}^{-2}$. Thus, there is a one order of magnitude reduction. In a multibeam bright-field TEM image, both screw- and edge-type dislocations are visible. Comparing the dark- and bright-field images of the vicinal film [Figs. 2(b) and 2(c), respectively], we identify only one screw in the area of view. Thus, the density of threading screw dislocations in the vicinal film is estimated to be $\sim 2 \times 10^7 \text{ cm}^{-2}$, which is consistent with the result from STM observations (i.e., less than 10^8 cm^{-2}). As mentioned earlier, in films grown on singular substrates, the density of screws is established by STM to be $2 \times 10^9 \text{ cm}^{-2}$ [from Fig. 1(b)], which is two orders of magnitude higher.

To explain the reduction of extended defects in the vicinal film, we recall that the 10^{10} cm^{-2} threading dislocation in the flat film is much higher than that in the substrate (i.e., less than 10^4 cm^{-2} according to Cree’s specification). Therefore, they must mostly originate from the nucleation and initial growth processes. In particular, screw dislocations arise from the coalescence of islands, which has reached a certain critical size during GaN growth.² On a vicinal substrate, by contrast, initial growth is by island nucleation on terraces *as well as* atomic incorporation at the step edges. The two processes thus compete for the arriving atoms. On narrow terraces, as is the case here where the average terrace width is only 100 \AA , growth fronts from the step edges soon coalesce with the nucleated islands before the islands reach the critical size and become misaligned. Once coalesced, the islands are incorporated into the growth fronts of the steps and this incorporation suppresses the development of growth errors such as screw dislocations. We have carried out stop-growth measurements at intervals of every few minutes. STM images show that after a 2.5 min deposition, growth fronts are seen in the form of flat-topped islands connected to step edges. Once the entire substrate surface is covered, further growth is by homoepitaxial step flow. At no deposition time do we observe spiral growth. Thus, the introduction of step edges as growth centers in a vicinal film is key to the dramatic reduction of screw dislocations in the vicinal film.

Photoluminescence (PL) and x-ray diffraction rocking-curve measurements confirm that the quality of the vicinal film is superior to the flat ones. For example, x-ray rocking curves from the vicinal films have a full width at half maximum (FWHM) of ~ 130 arcsec as opposed to ~ 250 arcsec from the flat films. Furthermore, PL spectra of vicinal layers show very weak ‘‘yellow’’ luminescence but strong and sharp band-edge peaks (FWHM ~ 10 meV at 4 K). These contrast the flat films where the PL spectra are dominated by ‘‘yellow’’ luminescence while band-edge emissions are

weak. An interesting question is that because 4H-SiC(0001) is nonisomorphic with 2H-GaN(0001), stacking mismatch boundaries (SMBs) (Refs. 9 and 10) will occur at the step edges. However, SMBs are short-distance vertical defects because they can be cured by overgrowth with the correct stacking sequence.¹¹ Our data in Fig. 1(b) support this assertion because all the steps are double bilayers, strong evidence that far from the interface, the GaN film is entirely of the wurtzite structure. Finally, we are investigating further reduction of edge-type dislocations in vicinal films using substrates with different off-cut angles and orientations.

The authors are grateful to N. Wang, X. F. Duan, and S. T. Lee for the TEM experiments. This work is supported in part by H.K. RGC Grant Nos. HKU7118/98P, 7117/98P, 260/95P, HKU CRCG Grant No. 10201825, U.S. DOE Grant No. DE-FG02-84ER 45076, and NSF Grant No. DMR-9972958.

- ¹X. J. Ning, F. R. Chien, P. Pirouz, J. W. Yang, and M. Asif Khan, *J. Mater. Res.* **11**, 580 (1996).
- ²X. H. Wu, P. Fini, E. J. Tarsa, B. Heying, S. Keller, U. K. Mishra, S. P. DenBaars, and J. S. Speck, *J. Cryst. Growth* **189/190**, 231 (1998).
- ³B. Heying, E. J. Tarsa, C. R. Elsass, P. Fini, S. P. DenBaars, and J. S. Speck, *J. Appl. Phys.* **85**, 6470 (1999).
- ⁴A. R. Smith, R. M. Feenstra, D. W. Greve, M. S. Shin, M. Skowronski, J. Neugebauer, and J. E. Northrup, *J. Vac. Sci. Technol. B* **16**, 2242 (1998).
- ⁵S. M. Seutter, M. H. Xie, W. K. Zhu, L. X. Zheng, Huasheng Wu, and S. Y. Tong, *Surf. Sci.* **445**, L71 (2000).
- ⁶M. H. Xie, S. M. Seutter, W. K. Zhu, L. X. Zheng, H. S. Wu, and S. Y. Tong, *Phys. Rev. Lett.* **82**, 2749 (1999).
- ⁷Y. Xin, S. J. Pennycook, N. D. Browning, P. D. Nellist, S. Sivanathan, F. Omnes, B. Beaumont, J. P. Faurie, and P. Gibart, *Appl. Phys. Lett.* **72**, 2680 (1998).
- ⁸F. A. Ponce, D. P. Bour, W. Götz, and P. J. Wright, *Appl. Phys. Lett.* **68**, 57 (1996).
- ⁹B. N. Sverdlov, G. A. Martin, H. Morkoc, and D. J. Smith, *Appl. Phys. Lett.* **67**, 2063 (1995).
- ¹⁰S. Tanaka, R. S. Kern, and R. F. Davis, *Appl. Phys. Lett.* **66**, 37 (1995).
- ¹¹J. E. Northrup, J. Neugebauer, and L. T. Romano, *Phys. Rev. Lett.* **77**, 103 (1996).